A NEW PM-ASSISTED SYNCHRONOUS RELUCTANCE MACHINE WITH A NONCONVENTIONAL FRACTIONAL SLOT PER POLE COMBINATION

Matteo Gamba, Gianmario Pellegrino and Alfredo Vagati
DENERG Politecnico di Torino, Corso Duca degli Abruzzi 24, 10129, Torino
Tel. +390110907143, Fax. +390110907199
matteo.gamba@polito.it, gianmario.pellegrino@polito.it, alfredo.vagati@polito.it

Abstract- *Fractional-slot concentrated-winding synchronous permanent magnet machines (PM) are appreciated for their simple construction and high torque density. Unfortunately, it is well known that such fractional slot / pole combinations kill the reluctance torque potential of salient interior PM rotor configurations. To date, this has hindered the application of fractional windings to machines of the Synchronous Reluctance and PM-assisted Synchronous Reluctance types. This paper proposes a new fractional slot PM-assisted Synchronous Reluctance machine with 24 slots and 10 rotor poles. The new machine is compared to a benchmark 10-pole PM-assisted machine having 90 slots and distributed windings and to another competitor with 12 slots concentrated windings. FEA results show that the new machine is comparable to the distributed windings version in terms of torque density and losses, and much easier to be manufactured.*

Keywords. *Synchronous Reluctance Machine, Variable Speed Drives, Permanent Magnet Synchronous Machine Drives, Fractional Slot Machines, Electrical Machines Comparison*

I. INTRODUCTION

Fractional-slot concentrated-winding permanent magnet (PM) machines are appreciated for their ease of manufacturing and short end connections. Modular construction can increase the slot filling factor resulting in very high torque density figures [1]. Different slot-versus-pole combinations and rotor configurations have been investigated and commercially applied [2], with rotors of the surface-mounted PM (SPM) or interior PM (IPM) [3] types. With fractional slots the armature flux linkage can be calibrated by design to match the PM flux linkage and obtain an infinite constant power speed range [4]. However, it has also been noticed that salient IPM rotors associated to fractional slot windings do not retain the expected reluctance torque contribution [5-6]. Thus, it is very rare in the literature that the Synchronous Reluctance (SyR) and the PM-assisted SyR (PM-SyR) machines have been realized with fractional-slot windings, because of such reluctance-killing effect of fractional slot configurations. The combination $q = 0.5$ is the only exception, being q the number of slots per pole per phase, which maintains saliency ratios sufficient for application to PM-SyR machines [7,8].

This paper proposes a new PM-SyR machine with a nonconventional 24 slot/10 pole fractional configuration. The 24/10 combination ($q = 4/5$) was recently proposed for SPM motors application [9]. It is derived from the popular 12 slot/10 pole combination ($q = 2/5$), aiming at reducing the harmonic content of the magneto-motive force (MMF) distribution. The 12/10 combination was chosen in [9] and here as the starting point because it is very popular in the literature, but similar transformations apply to other concentrated-winding configurations.

The proof of principle presented here shows that the 24/10 PM-SyR machine preserves the most of the reluctance torque of the salient rotor, opening the stage to a new class of fractional-slot SyR and PM-SyR solutions. In turn, the 24/10 PM-SyR machine retains most of the ease of manufacturing of fractional slots together with the advantages of PM-SyR rotor topologies, such as PM cost reduction [10-11], uncontrolled generator voltage reduction [12], higher power overload [12-13].

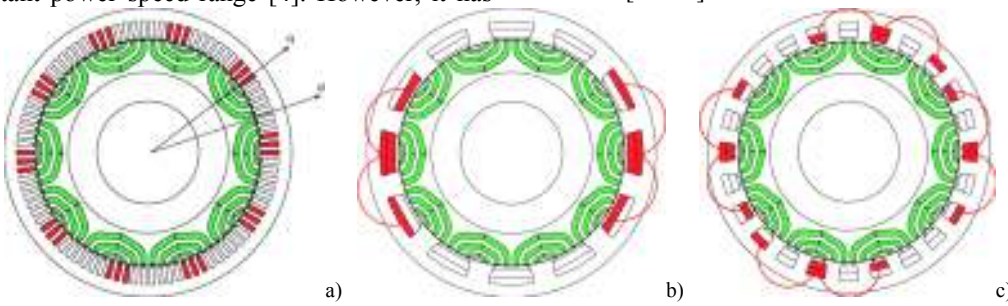

Fig 1. Cross sections of the three PM-SyR machines under analysis: a) q=3, distributed windings; b) q=2/5, concentrated windings; c) proposed q=4/5 solution, with mildly overlapping windings. The red areas in the slots indicate one phase. The end turns are also evidenced.

Three PM-SyR machines are compared in the paper, all having the same 10-poles rotor and the same stack outer dimensions. The first machine has 90 stator slots and standard distributed windings (q = 3). The second one has 12 slots with 12 tooth-wound coils (q = 2/5, double side), and the third machine is the new one, with a double layer winding housed in 24 slots and the end turns mildly overlapping (q = 4/5). The cross sections of the three machines are reported in Fig. 1. The green colored barriers account for the presence of the PM material. The PMs fill the rotor saliencies completely, as if plastic bonded magnets were used, but this is not necessarily the case in reality, as addressed in section III. The main data of the three machines are reported in Table I. At first the paper analyzes the reluctance torque performance, with no magnets in the rotors, to put in evidence the reluctance bases of the three configurations. Secondly, the PMs are inserted and the performance of the final PM-assisted machines is assessed and compared via finite element analysis (FEA) computation. As the reluctance effect is different for the three machines, also the PM quantity will be different for the three rotors, as will be commented.

TABLE I
MAIN FIGURES OF THE THREE MACHINES UNDER COMPARISON

Slots/pole/phase (q)		3	2/5	4/5
Number of phases (m)		3		
Stator slots (S)		90	12	24
Pole pairs (p)		5		
Turns in series per phase (N)		70		
Outer diameter (D)	[mm]	380		
Stack length (L)	[mm]	280		
Air gap (g)	[mm]	0.75		
Slot fill factor (k_{Cu})		0.4		
End winding length	[mm]	0.151	0.081	0.135
Phase resistance @ 130°C (R_s)	[Ohm]	0.117	0.100	0.114
End-winding resistance @ 130°C	[Ohm]	0.0393	0.0205	0.0354
Type of cooling		Forced ventilation		

II. SYNCHRONOUS RELUCTANCE PERFORMANCE

In this section, the machines are FEA simulated with no magnets in the rotors to segregate the reluctance torque and the armature dq flux linkages. The common 3-layer rotor was chosen for its good match with the q = 3 stator [14], but the conclusions of the analysis are valid also for other layer numbers. The same current level (120 Apk) and the same number of turns in series per phase are used in this section for the three SyR machines. It must be considered that the q = 3 machine has a higher winding factor (k_w = 0.96 versus 0.933 and 0.925), and that conversely the q = 2/5 machine has the shortest end turns. This to say that with the same current the q = 3 has a higher fundamental MMF, but the q = 2/5 recovers in terms of lower Joule losses. The results presented in this section show a first clear trend in terms of reluctance torque. A more accurate comparison of the PM-assisted performance is presented in IV, at same target torque.

A. Concentrated versus Distributed Windings

At first, the benchmark q = 3 motor and the concentrated windings configuration q = 2/5 are considered. The SyR rotor is designed according to the state of the art: the reluctance torque is maximized by the alternation of air barriers and steel segment widths [14-15]. The barrier ends are regularly displaced at the airgap, for torque ripple minimization. The rotor pitch was optimized for the q = 3 stator [14-16].

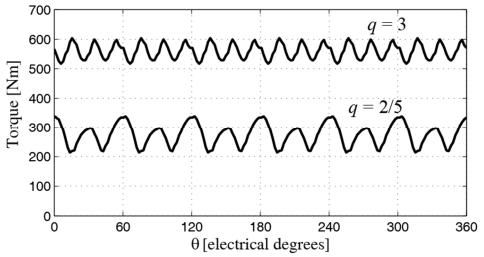

Fig 2. Torque waveforms of the q = 3 and the q = 2/5 machines at same current (120 Apk), over one electric period.

The torque waveforms at 120 Apk are reported in Fig. 2 for the two machines. The respective maximum torque per Ampere (MTPA) conditions were considered, FEA evaluated. The average torque values are 560 Nm and 275 Nm (49 %), and the peak to peak ripples are 80 Nm and 110 Nm (138%), respectively for the q = 3 and 2/5 machines. The torque ripple of the q = 3 has 18 cycles per electrical period, from the stator slots periodicity [14]. The main torque ripple harmonics of the q = 2/5 case are the 6th and the 12th orders, referred to one electrical period. The 12th order comes from the lowest common multiple of slots and poles, whereas the 6th order is expected when a salient rotor associated to this slot/pole combination [3]. The rotor was not specifically designed for the q = 2/5 stator, so the ripple could be mitigated with specific countermeasures [15]. However, the result of this section is the drastic difference in terms of average torque, that impacts the performance of the final PM-assisted machines.

B. Comparison of the Flux Linkage Curves

The dq flux linkage curves of the two machines are represented in Figs. 3 and 4, respectively. The q = 2/5 curves show lower values of d- flux linkage and higher values of q-flux linkage and a more evident cross-saturation. The dq reference frame is defined in Fig. 1a according to the SyR machine conventions, and will be used also for the PM-assisted machines.

The comparison of Figs. 3 and 4 gives important insights on the worse torque performance of the fractional slot machine. The flux linkage and current vector amplitudes are conveniently put in evidence in the torque expression:

$$T = \tfrac{3}{2} p \cdot \bar{\lambda}_{dq} \times \bar{\imath}_{dq} = \tfrac{3}{2} p \cdot |\lambda||i| \cdot \cos\phi \qquad (1)$$

Along with the power factor (PF) cosϕ. The steady-state vector diagrams of the two machines are represented in Fig. 5, for the sake of exemplification. The current and flux

linkage vectors are proportionate to the 120 A MTPA condition reported in Table II.

Respect to the distributed windings machine (Fig. 5a), the fractional slot machine (Fig. 5b, indicated with "prime" where different) has a lower *d*-axis and a higher *q*-axis flux linkage components. Both factors lower the output torque according to (1). The flux linkage amplitude $|\lambda_{SyR}'|$ is in fact smaller than the one of the benchmark machine $|\lambda_{SyR}|$, from the smaller *d*-component. The increase of the *q*- flux linkage component increases the flux phase angle δ' with respect to δ, thus reducing the PF and then, again, the torque (1).

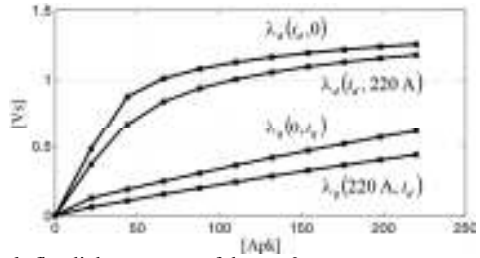

Fig 3. *dq* flux linkage curves of the $q = 3$ motor.

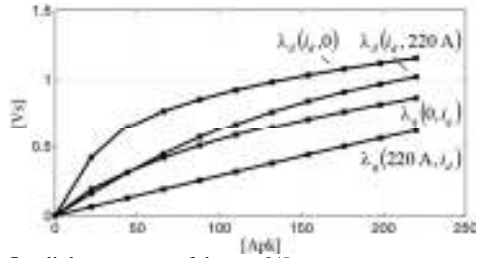

Fig 4. flux linkage curves of the $q = 2/5$ motor.

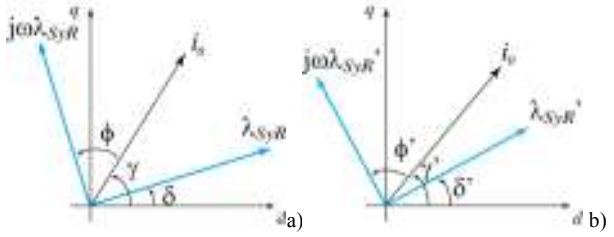

Fig 5. Steady-state *dq* vector diagram. a) $q = 3$ machine; b) $q = 2/5$ machine, with reduced *d*- and augmented *q*- flux linkages.

The lower *d*-axis flux linkage is to a minor extent related to the lower winding factor and primarily to the large slot openings of the 12-slot stator. If the slots were fictitiously made very narrow and with the same slot currents in, the *d*-flux linkage values of the $q = 2/5$ machine would become very close to the ones of the $q = 3$ machine, at least at zero i_q. Of course this is not feasible in practice because of the thermal constraints.

The large *q*-axis flux linkage of the $q = 2/5$ machine is a direct consequence of the fractional slot/poles combination, that vanishes the magnetic insulation effect of the multi-barrier rotor. When the phase currents are supplied according to the *q*-axis only, yet some rotor poles are offset from the insulation situation and subjected to MMF values that drive non-negligible flux through their flux guides. In other words, while the fundamental MMF component (order $5 = p$) is synchronous to the rotor and then correctly aligned with the rotor *q*-axis at all times, all non-synchronous MMF harmonics leak flux through the high-permeance flux guides. The insulation potential of the multi-barrier rotor is practically neutralized.

The flux leakage situation is exemplified in Fig. 6, where a *q*-axis only MMF is applied to the $q = 2/5$ machine. Poles 1 and 5 face the maximum MMF values and guarantee a good insulation, whereas poles 2 and 4 let the flux stream through their flux guides. Pole 3 is not subjected to MMF.

TABLE II
RESULTS OF THE MOTOR COMPARISON WITH NO PMS

Slots/pole/phase (q)		3	2/5	4/5
Current amplitude (i_0)	[Apk]	120		
Current phase angle (γ)	[deg]	58	50	55
Test speed	[rpm]	500		
d-axis flux linkage (λ_d)	[Vs]	0.90	0.72	0.87
q-axis flux linkage (λ_q)	[Vs]	0.28	0.39	0.36
Torque	[Nm]	560	275	457
Line to line voltage	[Vpk]	441	379	438
Power Factor		0.68	0.40	0.57

The evident cross-saturation of the $q = 2/5$ machine in Fig. 4 indicates that the two axes are poorly decoupled, much less than in the $q = 3$ case. In other words, the *q*-axis current has easy access to de-excite the *d*-axis channel and the same can be said for the *d*-axis current towards the *q*-axis flux linkage.

Fig 6. Field contour lines when *q*-axis mmf only is applied to 2/5 machine

III. PROPOSED 24 SLOTS/10 POLES SOLUTION

As said, the side effects of the 12/10 configuration come from the large slot openings and from the non-synchronous MMF harmonics. In the following, both effects will be mitigated by application of the 24 slot stator concept introduced in [9] for SPM synchronous motors.

A. 24/10 Winding Scheme

The 12-slots/12-coils winding is duplicated and the two half windings are phase-shifted by 2.5 slot pitches and then connected in series [9]. The phase shift of 2.5 pitches is chosen for the compensation of the 7-th harmonic. To make the half pitch displacement possible the slots are doubled and become 24. The process is graphically described in Fig. 7. The 24 slot/10 pole machine has $q = 4/5$. It is still a fractional slot/pole combination, but its end turns are mildly overlapped. The MMF spectrum of the $q = 4/5$ winding is reported in Fig.

8. The 7-th order is practically cancelled, along with orders 17, 31 and 41. Also the 1st order sub-harmonic is partially attenuated. Plus, the 24 slot stator has much smaller slot openings, and this enforces the *d*-axis flux linkage and increases the reluctance torque capability.

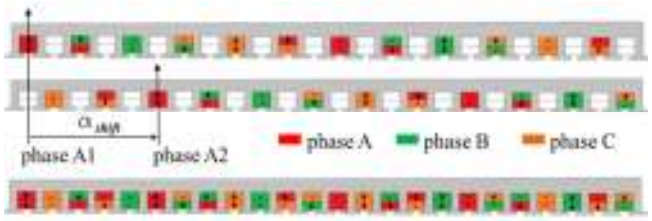

Fig 7. Construction of the 24 slots windings starting form two 12-slot windings.

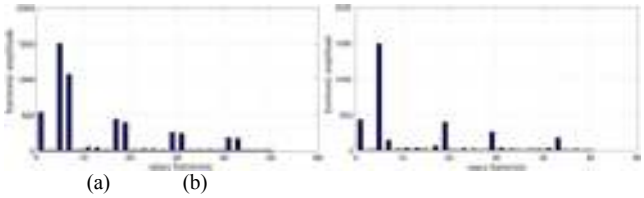

(a) (b)

Fig 8. MMF spectrum of the a) q = 2/5 machine and the b) q = 4/5 windings at 120 Apk.

B. Torque and Flux Linkage Comparison

The reluctance torque waveform of the q = 4/5 machine is FEA evaluated at 120 Apk, MTPA, and compared with the one of the q = 3 machine (Fig. 9). The average torque is 457 Nm which is 82% of the q = 3 benchmark, and 169% of the 270 Nm output by the q = 2/5 machine. The reluctance torque increase is encouraging. The peak to peak torque ripple amplitude is comparable to the q = 3 one, and its main component is the 6th harmonic in the electrical domain, 30th in the mechanical domain. Fig. 10 reports the *dq* flux linkage curves of the 24/10 SyR machine.

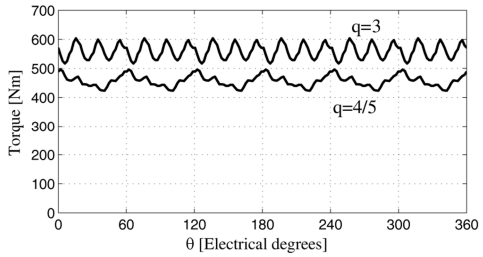

Fig 9. Torque of the q = 3 and the q = 4/5

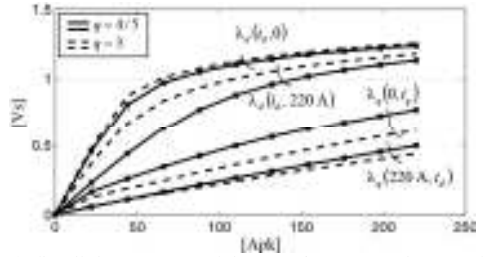

Fig 10. *dq* flux linkage curves of the q = 4/5 motor and comparison with the curves of the q = 3 benchmark.

As for the average torque, the behavior of the flux linkages is intermediate between the q = 3 and q = 2/5 situations, but promisingly closer to the former one. The *d*-axis flux linkage can reach the same levels of the distributed winding solution, but with a greater cross saturation effect that imposes larger i_d values to recover from the i_q related loss of excitation (*d*-axis) flux. The *q*-axis flux linkage is worse than in the q = 3 case and only slightly better than in the q = 2/5 case.

IV. PM Assisted Performance

The PMs are now designed for the three rotors individually with the goal of a common output target: the final PM-assisted machines give the same 670 Nm rated torque and have very similar corner speeds (between 465 rpm and 500 rpm).

A. PM Design for Natural Compensation

The PMs are designed in *natural compensation* conditions, i.e. the PM quantity and grade are chosen so that the PM flux linkage ideally compensates for the *q*-axis component of the armature flux linkage at rated current. The SyR style *dq* axes are adopted, as said. For the sake of modelling simplicity the flux barriers are filled with a plastic bonded PM material, whose remanence can be decided on a continuous basis by the designer. The remanence of the PM material is then a single design input able to trim the grade of PM assistance readily and with precision. The machines under investigation will require low values of such equivalent remanence (e.g. B_r = 0.18 T, 0.25 T). When dealing with the fabrication of real machines with commercial magnets (e.g. B_r = 0.36 T) the PM volumes will be reduced in inverse proportion to the increase of B_r, and machines with identical output figures will be obtained. In a way, the fictitious B_r used here for the design is also a useful indicator of the PM "equivalent quantity" needed in the three cases. The principle of natural compensation is shown in Fig. 11. Given the vector diagram of the initial SyR motor, the PMs are set for having zero flux linkage on the *q*-axis at rated current, in MTPA conditions. The process requires a couple of iterations before the exact torque value is associated to the zero *q*- flux linkage situation. The PM remanence is first evaluated by analytical formulas and then finalized with FEA simulation, for the three machines. The values of the equivalent B_r are reported in Table III.

B. PM-SyR Comparison at Same Torque

Table III reports different current values for the three machines, giving the same torque. In Fig. 12 the current vectors of the just designed PM-SyR machines are shown in the (i_d, i_q) current plane, each one in the respective MTPA conditions. The q = 3 and q = 4/5 cases have similar amplitudes (112 A and 121 A), whereas the q = 2/5 machine needs 158 A for its worse reluctance properties. Table III reports the *d*- and *q*- flux linkages figures for rated operating conditions. The *q*- flux linkage is close to zero by definition of natural compensation. The *d*- flux linkage values of the q = 3 and q = 4/5 designs are close to each other (0.954 Vs and 0.946 Vs, respectively) at the expense of a higher *d*-axis

current for the q = 4/5 (80 A versus 62.4 A), as expected from subsection III.B.

Despite the high i_d current (120 A), the q = 2/5 machine does not reach the same d- flux linkage value of the two competitors (λ_d = 0.877 Vs). A consequence of the smaller d-flux linkage is that also the q-current component must be increased, to get to the torque target. The result is that the current amplitude is a significant 158 A. Again, the penalty in terms of Nm per Ampere of this q = 2/5 PM-SyR machine comes from the low reluctance torque evidenced in Section II.

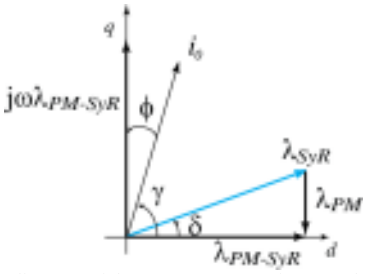

Fig 11. Vector diagram of the PM-SyR motor in natural compensation conditions.

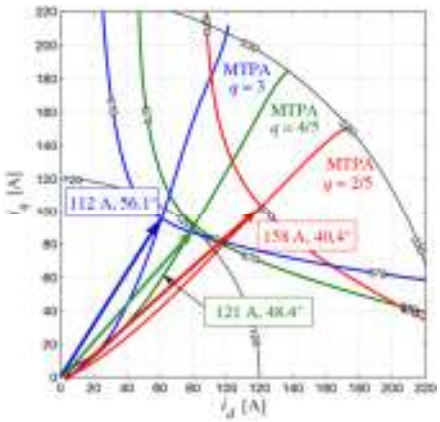

Fig 12. Current vectors of the three PM-SyR machines for the same output torque of 670 Nm. The respective MTPA curves are reported.

All the machines have 70 turns in series (Table I), and this is why the q = 2/5 ones has a slightly higher corner speed of 500 rpm versus the 465 rpm of the other two. If the former was rewound with 76 turns to have a corner speed of 461 rpm the current amplitude mismatch of Fig. 12 would be mitigated (146 Apk instead of 158 A, for 670 Nm). However, in this case the power-speed profile would become even worse than the one shown in Fig.15.

The rated torque waveforms are reported in Fig. 13 for the three machines, recalling the SyR ones of Figs. 2 and 10 in terms of torque ripple. The q = 3 and 4/5 machines have acceptable peak to peak ripple values, whereas the q = 2/5 one shows a very large ripple. As said, a specific rotor optimization could mitigate the problem. Yet, the proposed q = 4/5 solution is very competitive in this sense with no need for specific countermeasures, due to its improved MMF harmonic content and higher number of slots, with respect to the q = 2/5 case.

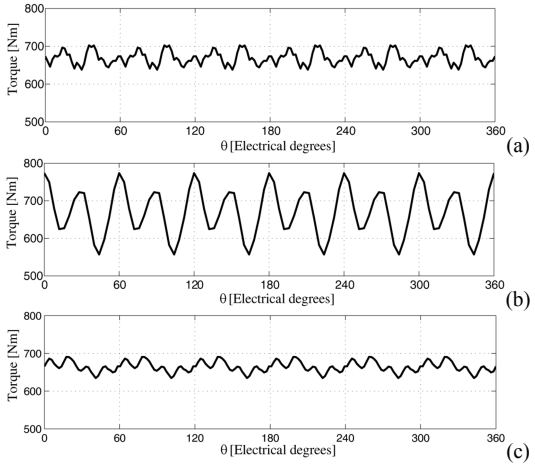

Fig 13. Rated torque waveforms of the three PM-SyR machines. a) q = 3; b) q = 2/5; c) q = 4/5.

C. *Power Versus Speed Curves*

The power versus speed curves at constant current amplitude and limited inverter voltage are reported for the three PM-SyR machines in Figs. 15 to 17. The order of the figures is q = 3, q = 2/5 and q = 4/5.

Each figure reports two power curves: one referring to the rated torque current (different for the three) and the second one referring to a common maximum value of 200 A (pk). All the power curves refer to a 400V dc-link. The rated torque and corner speed condition is indicated as *point A*. The maximum power at maximum speed is indicated as *point B*, and it is different for the three.

The power curves of the benchmark q = 3 and the proposed q = 4/5 machines are fairly close to each other. The maximum output power is 35 kW for the former and 30.5 kW for the latter. The maximum power conditions are 58 kW @ 500 rpm and 53 kW @ 500 rpm, respectively. According to the literature, flat power versus speed curves at constant current and limited voltage are facilitated by the presence of saliency, and vice-versa [12], and machines with more saliency have a higher power overload capability, with the same inverter limits [13]. The results of Figs. 14 to 16 are consistent with the literature in both senses, as the q = 3 machine is the one with the best SyR characteristics, followed by the q = 4/5 and, last, the q = 2/5 machine.

D. *Flux Linkage Comparison of the 24- and 12-Slot Machines*

The dq flux linkage curves of Figs. 18 and 19 summarize why it is convenient to pass from the q = 2/5 winding to the q = 4/5 one is given with the help of. The conclusions fairly reproduce the ones of Section II, where the SyR performance was analyzed. The key difference between the two PM-SyR machines is in their d-flux linkages (Fig. 17). It must be reminded that the d- component is the main flux linkage component, or the excitation one, so the one mostly influencing the output torque (1) through the flux-linkage amplitude. In natural compensation conditions the torque is strictly proportional to the d- flux linkage, because the q- flux component is zero. The q = 4/5 machine has higher values of

d-flux linkage at all (i_d, i_q) conditions, and a higher flux in saturation. This to say that even a strong increase of the i_d current could not compensate for the lower excitation flux level of the q = 2/5. More comments are in the Appendix.

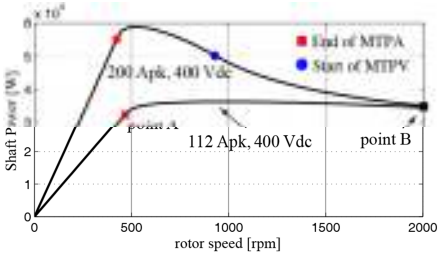

Fig 14. Power vs speed q=3 PMASR machines for two current level, 112A and 200A.

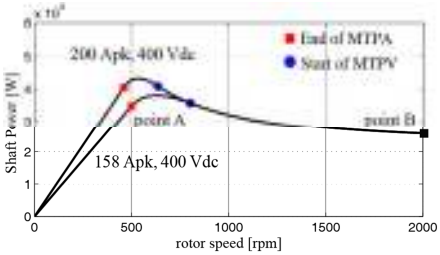

Fig 15. Power vs speed q=2/5 PMASR machines for two current level, 158A and 200A

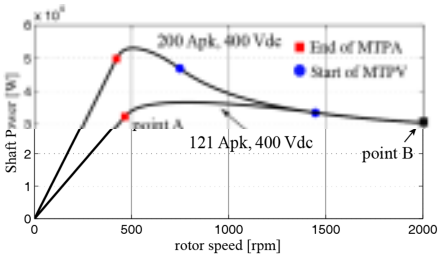

Fig 16. Power vs speed q=4/5 PMASR machines for two current level, 121A and 200A.

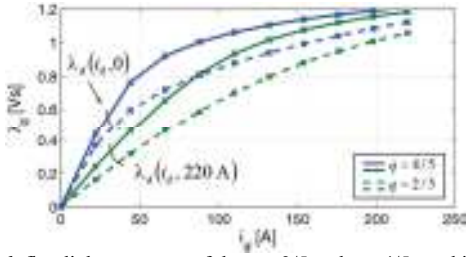

Fig 17. *d*- flux linkage curves of the q = 2/5 and q = 4/5 machines.

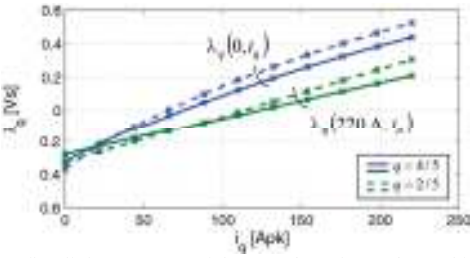

Fig 18. *q*- flux linkage curves of the q = 2/5 and q = 4/5 machines

The *q*- flux linkage curves in Fig. 18 point out the other minor improvement of the q = 4/5 solution. The PM flux linkage (i_d = i_q = 0) is nearly the same for the two machines, as also it is the effect of cross saturation. However, the slope of the q = 4/5 curves is lower than the one of the q = 2/5 curves, accounting for a lower *q*-axis inductance.

E. End turns and Copper Loss Comparison

The copper loss comparison is based on the stator phase resistance R_s formula:

$$R_s = \rho \cdot \frac{N^2}{2p \cdot q \cdot k_{Cu} \cdot A_{slot}} \cdot (l + l_{end}) \quad (2)$$

Where ρ is the resistivity of copper, N is the number of conductors in series per phase, k_{cu} is the slot fill factor, A_{slot} is the slot cross-sectional area, p number of poles, q number of slots per pole per phase, l and l_{end} are the stack and the end-turn lengths. The critical factors for this comparison are: 1) end-connection length, 2) slot fill factor and 3) operating temperature. This section addresses how the values of R_s reported in Table I were obtained.

A first formula was used for calculating the end-turn length of the overlapping windings (q = 3 and 4/5):

$$l_{end} = 2 \cdot l_t + \left(r + \frac{l_t}{2}\right) \cdot \alpha \quad (3)$$

Where r is the airgap radius and α is the angular span of the coil. For the q = 3, p = 5, full pitch winding it is:

$$\alpha = \frac{\pi}{p} = \frac{\pi}{5} \quad (4)$$

For q = 4/5 it is:

$$\alpha = 2 \cdot \alpha_{slot} = \frac{4\pi}{6qp} = \frac{\pi}{6} \quad (5)$$

These formulas refer to the model represented in Fig. 19.

A second formula is used for the concentrated windings, according to the scheme of Fig. 20, similar to the one used in [17]. The equation is:

$$l_{end} = \frac{1}{2} \cdot \left[w_t + \pi \cdot \left(r + \frac{l_t}{2}\right) \cdot sin\left(\frac{\alpha_{slot}}{2}\right)\right] \quad (6)$$

where α_{slot} is the slot angular pitch (π/6). The application of (3) and (6) leads to the l_{end} values in Table I: 151 mm for q = 3, 81 mm for q = 2/5, 135 mm for q = 4/5.

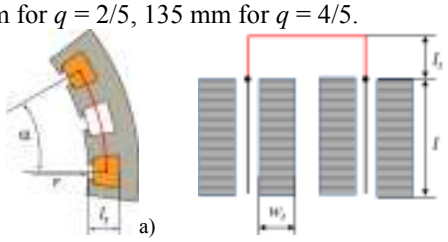

Fig 19. End-winding model used for q = 3 and q = 4/5. a) Frontal view; b) top-view cross section.

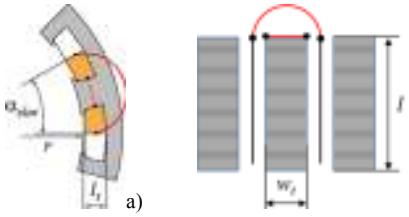

Fig 20. End-winding model used for q = 2/5. a) Frontal view; b) top-view cross section.

Another end-turn estimation taken from MotorSolve by Infolytica [18] gives more even results. This would say the proposed q = 4/5 is in between the other two machines: l_{end} = 130 mm for q = 3, 118 mm for q = 4/5 and 100 mm for q = 2/5. The 0.4 slot fill factor (net copper/gross slot area) for all is conservative for the tooth-wound q = 2/5 case, that could have higher figures. However, the equal fill factor partly balances the overestimated (3) and underestimated (6) end-turns, as just said.

Finally, the copper temperature set to 130°C for all is another coarse simplification. The three machines have different current levels, different phase resistances and most of all different slot size and layout. The narrower is the slot, the cooler will be the copper hot spot, thus q = 3 should be colder than q = 4/5, that should be colder than q = 2/5, also in case of same loss and same cooling. This is also confirmed by the thermal analysis run in MotorSolve.

A sound assessment of the Joule loss convenience of this new solution requires that prototypes are manufactured and tested, that is an ongoing activity.

F. Loss Comparison

The iron losses are FEA calculated at points *A* and *B* defined in Figs. 15 to 17, with Magnet by Infolytica [18]. The loss components at point *A* are reported in Fig. 21a, dominated by the copper losses. Although the distributed winding machine has the higher phase resistance, its copper loss is the minimum one, thanks to the smaller current amplitude. The q = 4/5 has 13% more copper loss, from the aggregate higher current and the slightly lower resistance. The tooth-wound machine despite of the lowest resistance has 63% more copper loss than the benchmark because of the high current. This high copper loss is unlikely compatible with continuous operation, if the same cooling setup is used for the three machines. Plus, if the equal copper temperature simplification is removed, the copper loss difference is even amplified by the different copper temperatures. The thermal analysis in MotorSolve reports a maximum copper temperature of 118°C for the q = 3, 144 °C for the q = 4/5 and 240 °C for the q = 2/5 case. As said, the latter looks dramatically inadequate, from the thermal point of view.

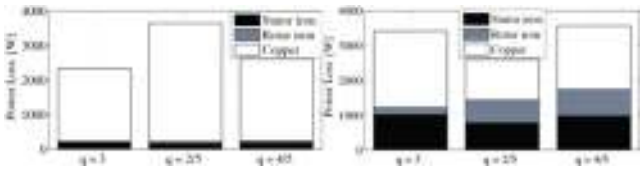

(a) (b)

Fig 21. Segregation of the loss component of the three PM-SyR machines at a) rated torque, base speed and b) maximum speed, maximum power (different for the three).

At maximum speed conditions (point *B*) the core loss are significant. For the fractional slot cases, also the ones on the rotor (Fig. 21b). The proposed q = 4/5 machine has the same rotor loss of the q = 2/5 one and the same stator loss of the q = 3 one. Copper loss may look a bit erratic in this figure, but it must be reminded that the three machines work at different current amplitudes, as a consequence of the MTPV limit, and produce different values of output power, as reported in Table III.

DISCUSSION

The points opened in the paper are summarized here:

- The popular combination 12/10 is not competitive for PM-assisted SyR machine applications.
- Its poor performance mainly comes from the slot openings, that are large with respect to the rotor pole pitch. Plus, the multi-barrier rotor insulation is ineffective due to non-synchronous harmonics.
- The proposed 24/10 machine can have a performance that is close to the one of the distributed winding benchmark, provided that a greater quantity of magnets is used (+39% in the examples, according to the remanence ratio).
- The improvements of the 24/10 respect to the 12/10 come from the smaller slot openings (versus the rotor pole pitch) and the polished MMF spectrum, that both increase the excitation flux linkage. The q- flux characteristic and the effectiveness of the insulation of the q- axis show minor improvements.
- The convenience in terms of end-winding length with respect to 90/10 is limited, due to the overlapping end-turns of the 24/10 windings. However, the copper loss reduction with respect to 12/10 is consistent, owing to the better Nm over Ampere coefficient.
- The core losses of the 24/10 machine are slightly worse than the ones of the two competitors.
- The proposed 24/10 machine is a promising tradeoff solution in terms of performance and ease of manufacturing, still maintaining a good flux weakening behavior.
- Other combinations [19] are under investigation, for improving the MMF harmonic content of fractional slots and retaining the tooth-wound feature.

CONCLUSION

This paper demonstrates that PM-SyR machines can be associated with success to specific fractional slot combinations such as the proposed 24/10 one. The presented 24/10 PM-SyR machine has torque and power figures that are comparable to the ones of the distributed windings benchmark. The proposed machine is easy to manufacture, even if not as advantageous as the tooth-wound coil ones. Further investigation is ongoing, in the directions of experimental validation and new slot – pole combinations.

APPENDIX: FIELD LINES WITH D CURRENT ONLY

The FEA results of Fig. 22 give an intuitive justification of the poor *d*-axis magnetization condition of the tooth-wound machine (q = 2/5). The benchmark machine (Fig. 23a) has the rotor poles uniformly exploited. The q = 2/5 machine (Fig. 23b) has one rotor pole which is unexcited and other two out of 5 partially exploited. This is visible also on the stator, partially unloaded. The proposed q = 4/5 solution (Fig. 23c)

has a good core exploitation, both on the stator and on the rotor.

TABLE III
COMPARISON OF THE PM-SYR MACHINES

Slots/pole/phase (q)		3	2/5	4/5
General Data				
PM remanence	[T]	0.18	0.25	0.25
Characteristic current	[A]	78	65	75
Open-circuit line to line voltage @ 2000 rpm	[Vpk]	417	406	409
Rated Torque and Speed Conditions (Point A)				
Corner speed	[rpm]	465	500	465
Torque	[Nm]	670	670	671
Current amplitude (i_0)	[Apk]	112	158	121
Current phase angle (γ)	[deg]	56.1	40.38	48.4
d-axis current (i_d)	[A]	62	120	80
q-axis current (i_q)	[A]	93	102	90
d-axis flux linkage (λ_d)	[Vs]	0.954	0.877	0.946
q-axis flux linkage (λ_d)	[Vs]	0.011	0.0088	-0.037
dc-link voltage	[V]	400		
Power Factor		0.941	0.91	0.935
Joule loss	[W]	2107	3426	2372
Maximum Speed (Point B), Steel Grade is M270-50				
Output Power	[W]	35000	25500	30500
Current amplitude	[Apk]	112 (*)	88 (*)	104 (*)
Copper Loss	[W]	2201	1172	1830
Stator iron loss	[W]	1007	771	971
Rotor iron loss	[W]	200	652	757

(*) the current amplitude is limited by the MTPV.

REFERENCES

[1] EL-Refaie, A.M., "Fractional-Slot Concentrated-Windings Synchronous Permanent Magnet Machines: Opportunities and Challenges," Industrial Electronics, IEEE Transactions on , vol.57, no.1, pp.107,121, Jan. 2010

[2] Cros, J., Viarouge, P., "Synthesis of high performance PM motors with concentrated windings," Energy Conversion, IEEE Transaction on, vol. 17, pp. 248-253, 2002.

[3] Bianchi, N.; Bolognani, S.; Pré, M.D.; Grezzani, G., "Design considerations for fractional-slot winding configurations of synchronous machines," Industry Applications, IEEE Transactions on , vol.42, no.4, pp.997,1006, July-Aug. 2006

[4] EL-Refaie, A.M.; Jahns, T.M., "Optimal flux weakening in surface PM machines using concentrated windings," Industry Applications Conference, 2004. 39th IAS Annual Meeting. Conference Record of the 2004 IEEE , vol.2, pp.1038,1047 vol.2, 3-7 Oct. 2004

[5] Reddy, P.B.; EL-Refaie, A.M.; Kum-Kang Huh; Tangudu, J.K.; Jahns, T.M., "Comparison of Interior and Surface PM Machines Equipped With Fractional-Slot Concentrated Windings for Hybrid Traction Applications," Energy Conversion, IEEE Transactions on , vol.27, no.3, pp.593,602, Sept. 2012

[6] Tangudu, J.K.; Jahns, T.M., "Comparison of interior PM machines with concentrated and distributed stator windings for traction applications," Vehicle Power and Propulsion Conference (VPPC), 2011 IEEE , pp.1,8, 6-9 Sept. 2011

[7] Murakami, H.; Kataoka, H.; Honda, Y.; Morimoto, S.; Takeda, Y., "Highly efficient brushless motor design for an air-conditioner of the next generation 42 V vehicle," Industry Applications Conference, 2001. Thirty-Sixth IAS Annual Meeting. Conference Record of the 2001 IEEE, vol.1, no., pp.461,466.

[8] Xiao Chen; Jiabin Wang; Lazari, P.; Liang Chen, "Permanent Magnet Assisted Synchronous Reluctance Machine with fractional-slot winding configurations," Electric Machines & Drives Conference (IEMDC), 2013 IEEE International, pp.374,381, 12-15 May 2013.

[9] Dajaku, G.; Gerling, D., "A Novel 24-Slots/10-Poles Winding Topology for Electric Machines," Electric Machines & Drives Conference (IEMDC), 2011 IEEE International, pp.65,70, 15-18 May 2011.

[10] Guglielmi, P.; Boazzo, B.; Armando, E.; Pellegrino, G.; Vagati, A., "Permanent-Magnet Minimization in PM-Assisted Synchronous Reluctance Motors for Wide Speed Range," Industry Applications, IEEE Transactions on , vol.49, no.1, pp.31,41, Jan.-Feb. 2013.

[11] Ooi, S.; Morimoto, S.; Sanada, M.; Inoue, Y., "Performance evaluation of a high power density PMASynRM with ferrite magnets," Energy Conversion Congress and Exposition (ECCE), 2011 IEEE , vol., no., pp.4195,4200, 17-22 Sept. 2011

[12] Pellegrino, G.; Vagati, A.; Guglielmi, P., "Design Tradeoffs Between Constant Power Speed Range, Uncontrolled Generator Operation, and Rated Current of IPM Motor Drives," Industry Applications, IEEE Transactions on , vol.47, no.5, pp.1995,2003, Sept.-Oct. 2011

[13] Pellegrino, G.; Vagati, A.; Guglielmi, P.; Boazzo, B., "Performance Comparison Between Surface-Mounted and Interior PM Motor Drives for Electric Vehicle Application," Industrial Electronics, IEEE Transactions on , vol.59, no.2, pp.803,811, Feb. 2012

[14] Vagati, A., Pastorelli, M., Francheschini, G., Petrache, S., "Design of low-torque-ripple synchronous reluctance motors," Industry Applications, IEEE Transactions on, vol. 34, no. 4, pp. 758 -765, Jul/Aug 1998.

[15] Alberti, L.; Barcaro, M.; Bianchi, N., "Design of a Low Torque Ripple Fractional-slot Interior Permanent Magnet Motor," Industry Applications, IEEE Transactions on , in Press.

[16] P. L. Alger, *Induction Machines,* 2nd ed. New York: Gordon and Breach, 1970

[17] N. Bianchi, M. Dai Pre, L. Alberti, and E. Fornasiero, "Theory and design of fractional-slot PM machines," in Conf. Rec. IEEE IAS Annu. Meeting, New Orleans, LA, Sep. 23, 2007.

[18] http://www.infolytica.com

[19] Dajaku, G.; Gerling, D., "A novel tooth concentrated winding with low space harmonic contents," Electric Machines & Drives Conference (IEMDC), 2013 IEEE International, pp.755,760, 12-15 May 2013.

Fig 22. Flux density contours for the three PM-SyR machines supplied with d-axis current only. a) q = 3; b) q=2/5; c) proposed q=4/5 solution.